JOURNAL OF Materials CHEMISTRY

The decomposition mechanism of *p*-chloromethylphenyltrimethoxysiloxane self-assembled monolayers on vacuum ultraviolet irradiation

Nagahiro Saito,* Kazuyuki Hayashi, Hiroyuki Sugimura and Osamu Takai

Department of Materials Processing and Engineering, Graduate School of Engineering, Nagoya University, Furo-cho, Chikusa, Nagoya 464-8603, Japan. E-mail: nagahiro@plasma.numse.nagoya-u.ac.jp

Received 15th April 2002, Accepted 10th June 2002
First published as an Advance Article on the web 19th July 2002

The decomposition mechanism of *p*-chloromethylphenyltrimethoxysiloxane (CMPS) self-assembled monolayers (SAMs) due to vacuum ultraviolet (VUV) irradiation at a wavelength of 172 nm has been studied based on water repellency, X-ray photoelectron spectroscopy (XPS) and Kelvin probe force microscopy (KPFM). The CMPS-SAMs were prepared through chemical vapor deposition at 100 °C. The water contact angle increased dramatically within the first 30 min, reaching a plateau at this point. The saturated water contact angle was 76°. Next, the CMPS-SAMs were irradiated at under 10 Pa from 0 to 30 min. The CMPS-SAMs irradiated for 15 and 30 min were covered with carboxylated hydrocarbon fragments and silanol groups, respectively. KPFM measurements for micro-patterned SAMs, *i.e.* CMPS/CO_2H and CMPS/SiOH, showed that the surface potential of the carboxylated and silanol regions were −16 and +19 mV *vs.* CMPS-SAM, respectively. The former negative surface potential difference originated in the electronegativity of the CO_2H fragments. These results provide us with a route to prepare an organic template for various fields such as bio-sensors, chemical sensors and electrolytes.

Introduction

Micropatterning of self-assembled monolayers (SAMs) is an attractive technique to produce organic templates for various microfabrication processes and molecular electronic devices.[1–4] The technique includes micro-contact printing,[5–8] scanning probe lithography[9–13] and photolithography.[14–17] Among these methods, photolithography is a promising technique from the viewpoints of industrial applications, since the method has a high-throughput and is readily applicable to large-area substrates.

A number of recent reports on photolithography of SAMs have been focused on the primary degradation pathway of alkanethiol SAMs.[18–22] In this chemistry, it is suggested that photo-generated ozone and/or its decomposition products attack the thiolate headgroups to produce solvent-labile species and cleavage of the C–S bond. On the other hand, the photodegradation of organosilane-SAMs have been less reported so far compared with those on alkanethiol SAMs. Ye *et al.*[23] investigated the photoreactivity of octadecylsiloxane (ODS) SAMs to ultraviolet (UV) light using water contact angle measurements, Fourier transform infrared spectroscopy (FT-IR) and atomic force microscopy (AFM). Their results suggested that, under UV irradiation, the main reactive sites of the alkylsiloxane SAMs were their hydrocarbon chains. They concluded that the SAMs were further attacked by OH radicals and atomic oxygen species, that is, the main products of UV dissociation of ozone molecules. Brandow *et al.*[24] investigated the surface modification of *p*-chloromethylphenyltrimethoxysiloxane (CMPS) SAMs with UV-irradiation at 190 nm. They succeeded in converting chloromethyl groups into aldehyde moieties. These aldehyde groups were further converted chemically to amino groups. The amino-terminated SAMs can be used as organic templates for binding biological materials.[25–27] However, few reports have been made on the photo-patterning of SAMs on irradiation with vacuum ultraviolet (VUV) light at wavelengths much shorter than 200 nm, particularly relating to reaction mechanisms. The principal advantage of VUV irradiation is that SAMs can be rapidly removed from substrates since the VUV light promotes cleavage of Si–C and C–C bonds and enables more detailed patterns to be obtained.

In order to establish a rapid and high-resolution lithography of CMPS-SAMs using a VUV lamp, we began to investigate photochemical reactions of CMPS-SAMs. We evaluated the decomposition of CMPS-SAM with VUV-irradiation time on the basis of water contact angle measurements, X-ray photoelectron spectroscopy (XPS) and Kelvin probe force microscopy (KPFM).

Experimental

Preparation of self-assembled monolayers

CMPS-SAMs were prepared on substrates of n-type silicon by chemical vapor deposition. Silicon substrates covered with a thin oxide layer (*ca.* 2 nm) were cleaned and hydroxylated simultaneously by a UV/ozone cleaning method.[28] The water contact angle of the silicon substrate changed from more than 40° before treatment to almost 0° afterwards since a thin oxide layer, whose surface was most likely terminated with OH groups, formed on the Si substrate. The cleaned samples were placed together with a galss cup filled with 0.2 cm^3 organosilane liquid [CMPS: Tokyo Kasei Organic Chemicals, $CH_2Cl(C_6H_4)$-$Si(OCH_3)_3$], into a 65 cm^3 Teflon® container. The container was sealed with a cap and placed in an oven maintained at 373 K for a set period. The reaction time was varied from 10 to 180 min. The CMPS liquid in the vessel vaporized and reacted with the OH groups on the sample surface. The molecules were fixed onto the sample surface and connected to adjacent CMPS molecules through siloxane bridges. The thickness of the saturated CMPS-SAM estimated by elipsometry was *ca.* 0.6 nm.

 DOI: 10.1039/b203643f

This journal is © The Royal Society of Chemistry 2002

Vacuum ultraviolet irradiation

In the VUV irradiation experiments, the surface was irradiated under a reduced pressure of 10 Pa with vacuum ultraviolet (VUV) light through a 10 mm quartz glass plate. The source of light employed in this study was an excimer lamp with λ = 172 nm (10 mW cm^{-2}, Ushio Electric, UER20-172V).

The water repellency of the obtained CMPS-SAM surfaces was evaluated by measuring their water contact angles through the sessile-drop method in air using an automatic contact anglemeter (CA-X150, Kyowa Interface Science).

X-Ray photoelectron spectroscopy

XPS (ESCA-3300, Shimadzu) measurements were performed under the following conditions. The Mg-Kα X-ray source was operated at 10 mA and 30 kV. All binding energies were referenced to metallic Si_{2p} at 99.34 eV, and intensities were normalized to the total Si_{2p} area. The take-off angle was 90°. The standard peaks[29] used in this study were Si–*C* = 284.22 eV and aromatic ring *C*=C = 284.7 eV in poly(phenylmethylsiloxane), $\mathit{C}H_2Cl$ = 287.03 eV in poly(2-chloroethylmethacrylate), hydrocarbon = 285.0 eV in poly(tetramethyleneglycol), $\mathit{C}H_2$–O–$\mathit{C}H_2$ = 286.4 eV in poly(vinylethylether) *C*HCl = 287.44 eV in chlorinated poly(vinyl chloride) and $\mathit{C}O_2$ = 288.91 eV in poly(methacrylate).

Kelvin probe force microscopy

All samples in this study were studied in a nitrogen atmosphere with a KPFM (Seiko Instruments Inc., SPA-300HV+SPI-3800N) using a gold-coated silicon cantilever whose resonance frequency and *Q*-factor were 25.56 kHz and approximately 180, respectively. The following details of the KPFM measurements were determined on the basis of our previous research.[30] The cantilever was vibrated at a frequency of 23.60 kHz. An a.c. bias voltage of 2 V at a frequency of 5 kHz was applied between the probe and sample. KPFM images of the sample surface were acquired at a probe scan rate of 0.2 Hz. Before the measurements were performed, the chamber was evacuated for 2 hours (after which time a pressure of *ca.* 10^{-4} Pa was reached) and filled with nitrogen.

Results and discussion

Fig. 1(a) shows the relationship between the water contact angle of the Si substrates and preparation time. The water contact angle increased dramatically within the first 30 min, while it reached a plateau after 30 min. This saturation of the increase in water contact angle shows that the growth of CMPS-SAM is terminated: *i.e.* the substrate was completely covered with CMPS-SAM. On the basis of this result, we determined the preparation time to be 60 min for the VUV-irradiation experiments. Fig. 1(b) demonstrates the change in water contact angle of the CMPS-SAM due to VUV-irradiation as a function of the irradiation time. The change in the water contact angle is divided into three regions labelled (a), (b) and (c) in Fig. 1. In region (a), the water contact angle decreases monotonously whereas in region (b) it remains almost constant at around 35°. In region (c), it begins to decrease again, approaching *ca.* 0°. This result is in contrast with the results reported previously on alkylsilane SAMs, whose water contact angles monotonously decreased down to 0° due to VUV-irradiation.[23,31]

In order to clearly elucidate the VUV-degradation mechanism of the CMPS-SAM, we analyzed the chemical structures of the VUV-irradiated CMPS-SAM samples by XPS. Fig. 2 shows C1s spectra at irradiation times of 0, 15 and 30 min along with the C1s spectrum of a VUV/ozone cleaned Si substrate. The spectrum of unirradiated sample consists of four peaks: Si–*C* (284.1 eV), *C*=C in aromatic ring (284.6 eV), $\mathit{C}H_2Cl$

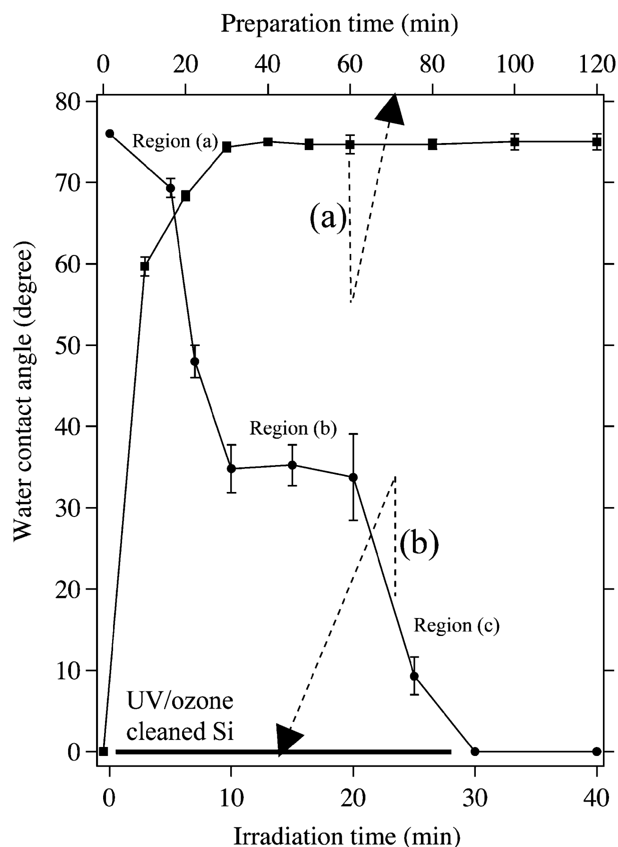

Fig. 1 Water contact angle of CMPS-SAM. (a) Water contact angle of the substrates treated with CMPS vapor at 373 K. (b) Relationship between water contact angle and VUV-irradiation time at a reduced pressure of 10 Pa.

(286.3 eV) and π–π* shake up peaks (289.8 eV). The peak for $\mathit{C}H_2Cl$ has a smaller binding energy than that of the standard peak. The origin of this peak shift is ascribable to the difference in the adjacent chemical structures between CMPS and the standard. In CMPS, the CH_2Cl group is attached to the aromatic ring, while the CH_2Cl groups in the standard are attached to a methylene group. The spectrum of the sample irradiated for 15 min consists of four components; Si–*C* (284.4 eV), hydrocarbon (285.0 eV), *C*HCl (287.5 eV) and $\mathit{C}O_2$ (289.4 eV). The Si–*C* peak for the sample is smaller than that of the unirradiated sample. This indicates that the organolayer has begun to be peel off from the existing siloxane networks at the bottom of the SAM. The peaks for *C*=C in the aromatic ring and $\mathit{C}H_2Cl$ of the unirradiated sample disappear, while those of hydrocarbon, $\mathit{C}O_2$ and *C*HCl become visible. Thus, the aromatic rings are converted into hydrocarbon fragments, which are partially oxidized and the CH_2Cl groups are converted into CHCl groups attached to the hydrocarbon fragments. The spectrum after irradiation for 30 min consists of two components; $\mathit{C}H_2$–O–$\mathit{C}H_2$ (286.0 eV) and $\mathit{C}O_2$ (288.3 eV). These peaks are attributable to organic contamination adsorbed from the atmosphere during the sample was transferred from the VUV-irradiation chamber to the XPS system, since the C1s peak intensity was approximately equal to that of a bare silicon wafer. According to these results, we presume the following photodegradation mechanism for CMPS-SAM. In region (a), the chlorine atoms are desorbed and then the aromatic rings decompose to hydrocarbon fragments. The desorbed chlorine atoms then attach to the hydrocarbon fragments. Furthermore, the hydrocarbon fragments at the sample surface are oxidized through chemical reactions with atomic oxygen species or OH radicals which are generated by the VUV-irradiation of atmospheric oxygen and water molecules. This might result in the

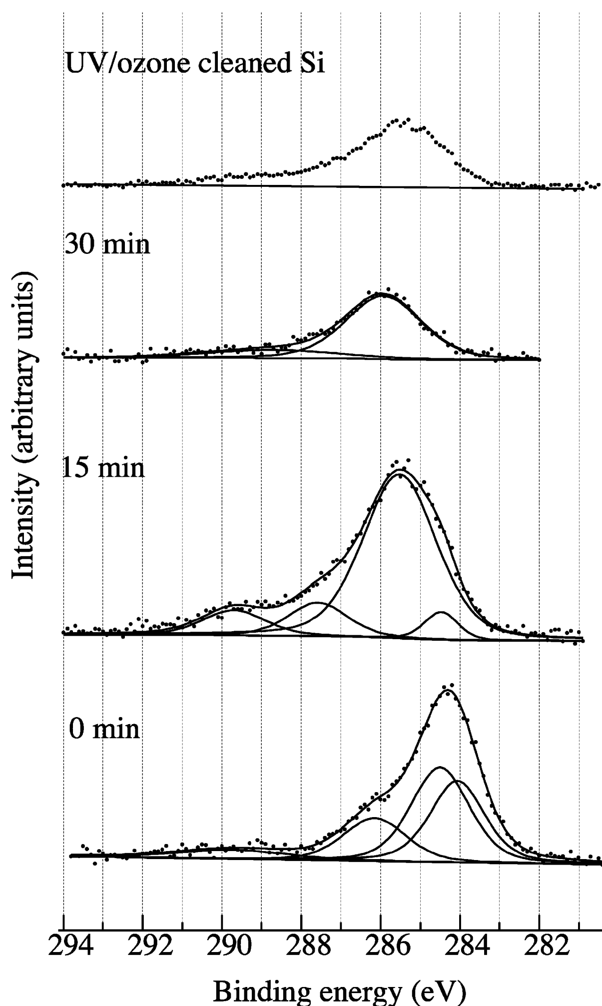

Fig. 2 C1s spectra of XPS for VUV irradiation times of 0, 15 and 30 min.

sample surface being covered with CO_2H and/or CHO groups. The water contact angle of an organic monolayer bearing CO_2H groups was reported as *ca.* 35°,[32] which agrees with that in region (b). In this region, the water contact angles of the samples are almost constant irrespective of the VUV-irradiation time. It can be explained from the decomposition reaction of the hydrocarbon fragments and the association reaction with chlorine atoms. These reactions alternately proceed like a radical chain reaction so that the water contact angles were apparently kept constant. However, the thickness of the stacked hydrocarbon layer decreases with as the reactions progress. Consequently, the water contact angle begins to decrease again and eventually the sample surface is covered with silanol groups after all the hydrocarbon layers have been removed; region (c).

There are two peaks located at 200.8 and 202.8 eV in the Cl2p spectra of the SAMs irradiated for 0 and 15 min. These peaks correspond to those of $Cl2p_{2/3}$ and $Cl2p_{1/2}$. The intensities of the sample irradiated for 15 min considerably weaken as compared to those of the as-deposited sample. There was no peak in the spectra of the samples irradiated for 30 min. This indicates that chorine disappeared during the initial stage of decomposition. In the Si2p spectra, two peaks attributed to SiO_2 and Si were observed. The ratio of the intensities (I_{SiO_2}/I_{Si}) became greater with increasing VUV irradiation time. The ratios at 0, 15 and 30 min were 0.27, 0.40 and 0.43, respectively. This change is thought to originate from two factors. In the as-deposited sample, the siloxane layer was incompletely formed since the dehydration between precursor molecules and silanol groups did not proceed efficiently.[33] Thus the intensity of SiO_2 increases since such the partially grown siloxane layer was

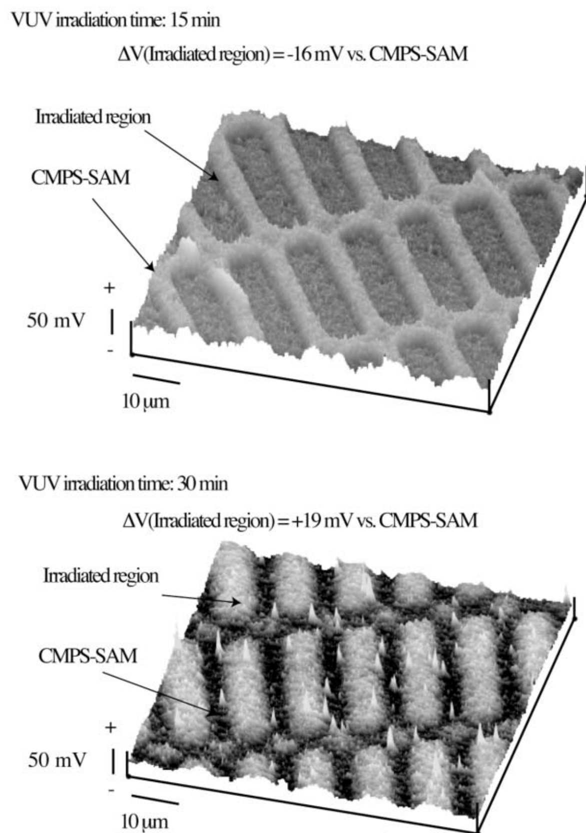

Fig. 3 KPFM images of CMPS-SAMs irradiated for 15 and 30 min through a photomask.

converted into SiO_2 by VUV irradiation. The results derived from Cl2p and Si2p spectra are consistent with the results obtained from C1s spectra.

Fig. 3 shows surface potential images of CMPS-SAMs irradiated through a photomask at 15 and 30 min, that is, the regions (b) and (c). The surface potential image of the sample irradiated for 15 min has two different regions showing more positive and negative potentials. The more positive and negative regions correspond to unirradiated and irradiated areas, respectively. The surface potential of the irradiated region was −16 mV *vs.* the value of the unirradiated one. The irradiated and unirradiated regions are considered to be covered with CO_2H-terminated hydrocarbon fragments and CMPS-SAM on the basis of XPS results, respectively. The origin of the surface potential difference is that the CO_2H fragments have a larger electronegativity than that of the CMPS-SAM. The surface potential image irradiated for 30 min also had two different regions. The more positive and negative potential regions correspond to irradiated and unirradiated ones, respectively. The surface potential of the irradiated region was +19 mV *vs.* the value of the unirradiated one. The irradiated region is terminated with silanol groups. Thus, the electronegativity of the silanol group is likely to be smaller than that of the CH_2Cl group.

Finally, we propose the decomposition mechanism for CMPS-SAM due to VUV irradiation at 172 nm to occur as schematically illustrated in Fig. 4. The chlorine atoms are desorbed and the aromatic rings are destroyed [region (a)]. The aromatic rings are converted to hydrocarbon fragments [region (b)] which are partially oxidized resulting in the formation of CO_2H groups on the sample surface. The desorbed chlorine atoms are attached to the hydrocarbon fragments and their oxidized forms. The decomposition reaction of the hydrocarbon fragments and the associated reaction with atomic oxygen or OH radicals alternately occur in a radical chain

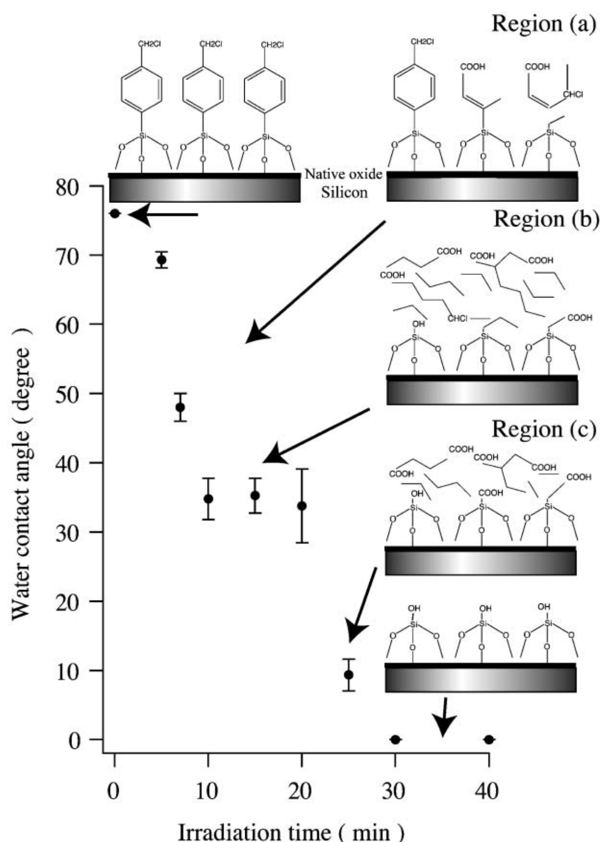

Fig. 4 Proposed decomposition mechanism of CMPS-SAM on VUV-irradiation.

reaction. During this step, the sample surface is covered with $-CO_2H$ groups leading to the constant water contact angles observed. However, the thickness of the hydrocarbon layer decreases with as the process progresses. All the hydrocarbon layers are finally removed and, consequently, the sample surface is terminated with silanol groups [region (c)]. This scheme also agrees with the change in surface potential of CMPS-SAM due to VUV-irradiation.

Conclusion

We have revealed the photochemical decomposition mechanism of CMPS-SAM with a VUV lamp at a wavelength of 172 nm based on water contact angle measurements, XPS and KPFM. We found that different VUV-irradiation times for CMPS-SAM provided us with two types of surface covered with different functional groups, *i.e.* CO_2H and SiOH. The KPFM images of micro-patterned SAMs (CMPS/CO_2H and CMPS/SiOH) showed that the surface potential in the CO_2H region was higher than that in the CMPS-SAM and that in the SiOH region was lower, *i.e.* we have a route for preparing functionalized templates with different surface potentials. This process is likely to be applied as the template for biosensors and molecular devices.

Acknowledgements

This work has been supported by the Research Project "Biomimetic Materials Processing" (no. JSPS-RFTF 99R13101) and the Research for the Future (RFTF) program of the Japanese Society for the Promotion of Science.

References

1 A. Ulman, *An Introduction to Ultrathin Organic Films*, Academic Press, Boston, MA, 1991.
2 A. Kumar, N. L. Abbott, E. Kim, H. A. Biebuyck and G. M. Whitesides, *Acc. Chem. Res.*, 1995, **28**, 219.
3 A. Bishop and R. G. Nuzzo, *Curr. Opin. Colloid Interface Sci.*, 1996, **1**, 127.
4 A. Ulman, *Chem. Rev.*, 1996, **96**, 1533.
5 A. Kumar and G. M. Whitesides, *Science*, 1994, **263**, 60.
6 Y. Xia and G. M. Whitesides, *J. Am. Chem. Soc.*, 1995, **117**, 3274.
7 N. L. Jeon, W. Lin, M. K. Erhardt, G. S. Girolami and R. G. Nuzzo, *Langmuir*, 1997, **13**, 3833.
8 H. X. He, H. Zhang, Q. G. Li, Q. T. Zhu, S. F. Y. Li and Z. F. Liu, *Langmuir*, 2000, **16**, 3846.
9 C. B. Ross, L. SUN and R. M. Crooks, *Langmuir*, 1993, **9**, 632.
10 C. R. K. Marrian, F. K. Perkins, S. L. Brandow, T. S. Koloski, E. A. Dobisz and J. M. Calvert, *Appl. Phys. Lett.*, 1994, **64**, 390.
11 M. J. Lercel, G. F. Redinbo, H. G. Craighead, C. W. Sjeen and D. L. Allara, *Appl. Phys. Lett.*, 1994, **65**, 974.
12 H. Sugimura and N. Nakagiri, *Langmuir*, 1995, **11**, 3623.
13 H. Sugimura and N. Nakagiri, *J. Am. Chem. Soc.*, 1997, **119**, 9226.
14 C. S. Dulcey, J. H. Georger, V. Krauthamer, D. A. Stenger, T. L. Fare and J. M. Calvert, *Science*, 1991, **252**, 551.
15 W. J. Dressick and J. M. Calvert, *Jpn. J. Appl. Phys.*, 1993, **32**, 5829.
16 N. Ichinose, H. Sugimura, T. Uchida, N. Shimo and H. Masuhara, *Chem. Lett.*, 1993, **11**, 1961.
17 N. Saito, K. Hayashi, H. Sugimura, O. Takai and N. Nakagiri, *Chem. Phys. Lett.*, 2001, **349**, 172.
18 M. M. Ferris and K. L. Rowlen, *Appl. Spectrosc.*, 2000, **54**, 664.
19 M. Lewis, M. Tarlov and K. Carron, *J. Am. Chem. Soc.*, 1995, **117**, 9574.
20 Y. M. Zhang, R. H. Terrill, T. A. Tanzer and P. W. Bohn, *J. Am. Chem. Soc.*, 1998, **120**, 2654.
21 K. L. Norrod and K. L. Rowlen, *J. Am. Chem. Soc.*, 1998, **120**, 2656.
22 G. E. Poirier, T. M. Herne, C. C. Miller and M. J. Tarlov, *J. Am. Chem. Soc.*, 1999, **121**, 9703.
23 T. Ye, D. Wynn, R. Dudek and E. Borguet, *Langmuir*, 2001, **17**, 4497.
24 S. L. Brandow, M. S. Chen, R. Aggarwal, C. S. Dulcey, J. M. Calvert and W. J. Dressick, *Langmuir*, 1999, **15**, 5429.
25 A. G. Frutos, J. M. Brockman and R. M. Corn, *Langmuir*, 2000, **16**, 2192.
26 V. Silin, H. Weetall and D. J. Vandearah, *J. Colloid Interface Sci.*, 1997, **185**, 94.
27 Z. Yang, W. Frey, T. Oliver and A. Chilkoti, *Langmuir*, 2000, **16**, 1751.
28 A. Hozumi, K. Ushiyama, H. Sugimura and O. Takai, *Langmuir*, 1999, **15**, 7600.
29 G. Beanson and D. Briggs, *High Resolution XPS of Organic Polymers The Scenta ESCA300 Database*; John Wiley & Sons, Chichester, UK, 1992.
30 H. Sugimura, K. Hayashi, N. Saito, O. Takai and N. Nakagiri, *Jpn. J. Appl. Phys.*, 2001, **40**, 4373.
31 H. Sugimura, T. Shimizu and O. Takai, *J. Photopolym. Sci. Technol.*, 2000, **13**, 69.
32 J. Drelich, J. L. Wilbur, J. D. Miller and G. M. Whitesides, *Langmuir*, 1996, **12**, 1913.
33 R. Maoz, J. Sagiv, D. Degenhardt, H. Mohwald and P. Quint, *Supramol. Sci.*, 1995, **2**, 9.